Single-Step Synthesis of Quantum Dots with Chemical Composition Gradients

Wan Ki Bae,[†] Kookheon Char,*[,†] Hyuck Hur,[‡] and Seonghoon Lee*[,‡]

School of Chemical and Biological Engineering, NANO Systems Institute, National Core Research Center, and School of Chemistry, NANO Systems Institute, National Core Research Center, Seoul National University, Seoul 151-747, Korea

Received March 19, 2007. Revised Manuscript Received October 9, 2007

We demonstrate a single-step synthetic method for highly luminescent (i.e., quantum yield up to 80%) and stable quantum dots (QDs) by using the reactivity difference between Cd and Zn precursors and that between Se and S precursors. A wide range of emission wavelengths (500−610 nm) with a narrow fwhm (<35 nm) is obtained by changing the ratios of the precursors. Under the reaction conditions selected, Cd- and Se (with a bit of S)-based cores are formed first and Zn- and S-based shells are formed successively; therefore, the QDs have a core/shell structure with composition gradients, which relieve the lattice mismatch between core and shells. The QDs are characterized using the combined techniques of HR-TEM, UV–vis, PL spectroscopy, and ICP-AES. The QDs also have energy gradients depending on their compositions in a radial direction, which energetically confine carriers (electrons and holes) to the cores. This leads to the stability of QDs during their surface passivation from oleic acid to mercaptopropionic acid and ensures their processibility for further purposes such as optoelectronic and biological applications.

Introduction

Quantum dots have received great attention for the past 10 years because of their unique electrical and optical properties that depend on their size and shape, which is termed the "quantum confinement effect (QCE)".[1–4] Because of their superb optical properties, they have been actively applied to light-emitting diodes,[5–8] lasers,[9–11] and biomarkers.[12–14] Although QDs are regarded as promising materials for optoelectronic devices and biological applications, synthetic methods developed so far have not been quite satisfactory, owing to their instability of photoluminescence (PL) in certain conditions.[14] As a result, several synthetic techniques were developed to produce highly luminescent and stable QDs via the surface modification using inorganic layers[15–19] or organic layers.[21–23] For example, the surface modification with inorganic layers has first been presented for the core/shell (CdSe/ZnS) structure with a discrete interface.[15] However, as the thickness of the shell layer is increased in order to enhance the chemical stability for further applications, the quantum efficiency starts to decline after a certain thickness due to the defects in the shell induced by the lattice mismatch between the core and shell layers, the nonuniform growth of the shell, and the formation of grain boundaries between small clusters in the shell. In order to improve the structural stability and quantum efficiency, a multishell structure was developed through the formation of shell layers such as CdS,[16] ZnSe,[17] and alloy shell layers between the CdSe core and the ZnS shell[19] using multireaction steps.

Surface passivation with organic layers was also developed to grow QDs with high quantum efficiency and narrow size

* Corresponding authors: e-mail khchar@plaza.snu.ac.kr, shnlee@snu.ac.kr.
† School of Chemical and Biological Engineering.
‡ School of Chemistry.

(1) Brus, L. *J. Phys. Chem.* **1986**, *90*, 2555–2560.
(2) Murray, C. B.; Kagan, C. R.; Bawendi, M. *G. Annu. Rev. Mater. Sci.* **2000**, *30*, 545–610.
(3) Weller, H. *Angew. Chem., Int. Ed. Engl.* **1993**, *32*, 41–53.
(4) Alivisatos, A. P. *Science* **1996**, *271*, 933–9377.
(5) Colvin, V. L.; Schlamp, M. C.; Alivisatos, A. P. *Nature (London)* **1994**, *370*, 354–357.
(6) Coe, S.; Woo, W. K.; Bawendi, M.; Bulovic, V. *Nature (London)* **2002**, *420*, 800–803.
(7) Achermann, M.; Petruska, M. A.; Kos, S.; Smith, D. M.; Koleske, D. D.; Klimov, V. I. *Nature (London)* **2004**, *429*, 642–646.
(8) Jun, S.; Jang, E.; Park, J.; Kim, J. *Langmuir* **2006**, *22*, 2407–2410.
(9) Klimov, V. I.; Mikhailovsky, A. A.; Xu, S.; Malko, A.; Hollingsworth, J. A.; Leatherdale, C. A.; Eisler, H. J.; Bawendi, M. G. *Science* **2000**, *290*, 314–317.
(10) Kazes, M.; Lewis, D. Y.; Ebenstein, Y.; Mokari, T.; Banin, U. *Adv. Mater.* **2002**, *14*, 317.
(11) Malko, A. V.; Mikhailovsky, A. A.; Petruska, M. A.; Hollingsworth, J. A.; Htoon, H.; Bawendi, M. G.; Klimov, V. I. *Appl. Phys. Lett.* **2002**, *81*, 1303–1305.
(12) Bruchez, M.; Moronne, M.; Gin, P.; Weiss, S.; Alivisatos, A. P. *Science* **1998**, *281*, 2013–2016.
(13) Chan, W. C. W.; Nie, S. M. *Science* **1998**, *281*, 2016–2018.
(14) Medintz, I. L.; Uyeda, H. T.; Goldman, E. R.; Mattoussi, H. *Nat. Mater.* **2005**, *4*, 435–446.
(15) Dabbousi, B. O.; Rodriguez-Viejo, J.; Mikulec, F. V.; Heine, J. R.; Mattoussi, H.; Ober, R.; Jensen, K. F.; Bawendi, M. G. *J. Phys. Chem. B* **1997**, *101*, 9463–9475.
(16) Li, J. J.; Wang, Y. A.; Guo, W.; Keay, J. C.; Mishima, T. D.; Johnson, M. B.; Peng, X. *J. Am. Chem. Soc.* **2003**, *125*, 12567–12575.
(17) Reiss, P.; Bleuse, J.; Pron, A. *Nano Lett.* **2002**, *2*, 781–784.
(18) Talapin, D. V.; Mekis, I.; Gotzinger, S.; Kornowski, A.; Benson, O.; Weller, H. *J. Phys. Chem. B* **2004**, *108*, 18826–18831.
(19) Xie, R.; Kolb, U.; Li, J.; Basche, T.; Mews, A. *J. Am. Chem. Soc.* **2005**, *127*, 7480–7488.
(20) Song, K.-K.; Lee, S. *Curr. Appl. Phys.* **2001**, *1*, 169–173.
(21) Qu, L.; Peng, X. *J. Am. Chem. Soc.* **2002**, *124*, 2049–2055.
(22) Talapin, D. V.; Rogach, A. L.; Kornowski, A.; Haase, M.; Weller, H. *Nano Lett.* **2001**, *1*, 207–211.
(23) Wuister, S. F.; Houselt, A.; Donega, C.; Vanmaekelbergh, D.; Meijerink, A. *Angew. Chem., Int. Ed.* **2004**, *43*, 3029–3033.

10.1021/cm070754d CCC: $40.75
Published on Web 01/01/2008

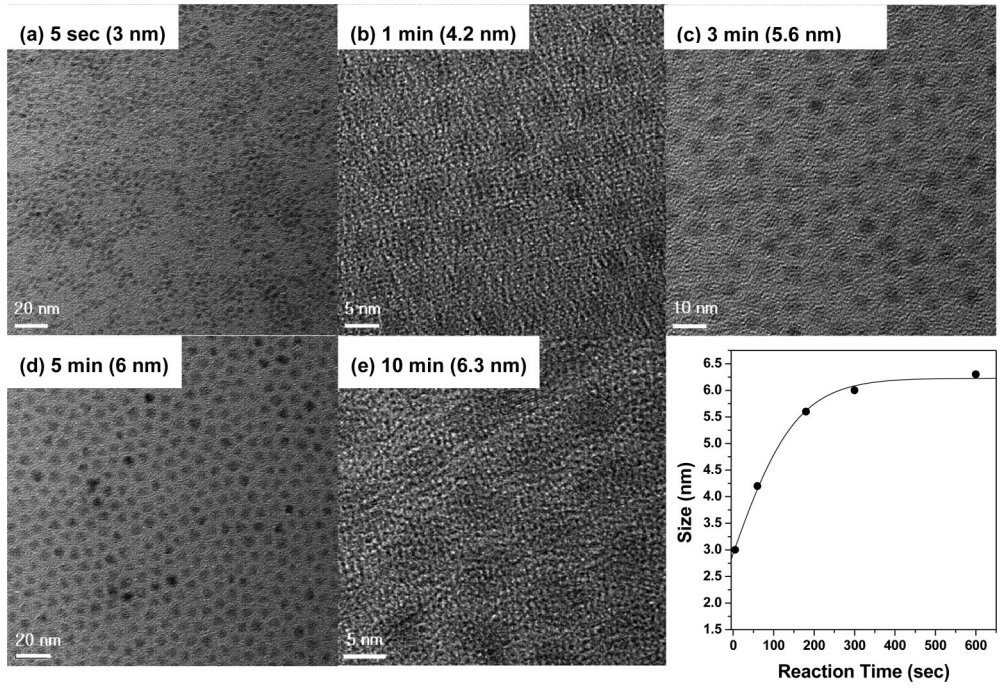

Figure 1. HR-TEM images of quantum dots as a function of reaction time: (a) 5 s, (b) 1 min, (c) 3 min, (d) 5 min, and (e) 10 min.

distribution, which were achieved with a variety of surfactants containing different functional groups such as trioctylphosphine oxide (TOPO),[15] hexadecylamine (HDA),[21] and their mixture.[22] Even though the enhancement of the quantum yield of QDs has been achieved, the synthesis of highly luminescent and structurally stable QDs in a large quantity and reproducible way still remains as a challenge due to difficulty in controlling the nucleation and growth in a synthetic process, which leads to a broad size distribution. Furthermore, the organic surfactants coordinated to the outermost surface of QDs must be removed for further optoelectronic applications.

Here, we present a single-step synthesis of highly luminescent quantum dots (i.e., quantum yield up to 80%) with a narrow fwhm (<35 nm) in a wide range of emission wavelengths (500−610 nm). The QDs prepared in the single-step synthesis are also structurally stable due to the chemical composition (or energy level) gradient in the radial direction, which effectively relieves the lattice mismatch and confines electrons and holes within the core. Moreover, since this single-step synthesis method requires at most two surfactants (oleic acid and trioctylphosphine), it is a straightforward, simple, reproducible, and economic method to obtain a large quantity of highly luminescent and structurally stable QDs.

Experimental Section

Chemicals. Cadmium oxide (CdO, 99.99%), zinc acetate (99.9%, powder), selenium (99.9%, powder), sulfur (99.9%, powder), trioctylphosphine (TOP, 90%), oleic acid (OA, 90%), 1-octadecene (ODE, 90%), and mercaptopropionic acid (MPA, 99.8%) were used as purchased from Aldrich.

Single-Step Synthesis of Quantum Dots with Chemical Composition Gradients. As a typical synthetic procedure, 0.4 mmol of CdO, 4 mmol of zinc acetate, 17.6 mmol of oleic acid, and 20 mL of 1-octadecne were placed in a 100 mL round flask. The mixture was heated to 150 °C, degassed under 100 mTorr pressure for 20 min, filled with N_2 gas, and further heated to 310 °C to form a clear solution of $Cd(OA)_2$ and $Zn(OA)_2$. At this temperature, 0.4 mmol of Se powder and 4 mmol of S powder both dissolved in 3 mL of TOP were quickly injected into the reaction flask. After the injection, the temperature of the reaction flask was set to 300 °C for promoting the growth of QDs, and it was then cooled to room temperature to stop the growth. QDs were purified by adding 20 mL of chloroform and an excess amount of acetone (3 times); they were then redispersed in chloroform or hexane. In order to tune the optical properties of QDs, we changed the ratios of Cd to Zn and Se to S with the total concentrations of the Cd−Zn pair and Se−S pair fixed at 4.4 mmol, while we maintained all the other parameters such as the amounts of OA, ODE, or TOP, reaction temperature, and reaction time constant.

Preparation of Water-Soluble Quantum Dots. Water-soluble quantum dots were prepared by replacing the OA attached to the surface of QDs with mercaptopropionic acid (MPA) as follows: 10 mg of QDs dispersed in 10 mL of chloroform was placed in a 100 mL round flask, and 2 mL of MPA was added to the solution. The resulting reaction mixture was heated up to 60 °C for 1 h and cooled to room temperature. The MPA-capped QDs were extracted by centrifugation at 6000 rpm, purified twice with chloroform, and finally dissolved into water of pH 8. We note that the MPA-capped QDs were water-soluble.

Optical Characterization. Room temperature UV–vis absorption spectra were measured with an Agilent 8454 UV–vis diode array spectrometer. Photoluminescence (PL) and photoluminescence excitation (PLE) spectra were collected on an ACTON spectrometer. The fluorescent quantum yield (QY) of the quantum dots prepared was measured and estimated by comparing their fluorescence intensities with those of primary standard dye solutions (with emission close to the QDs) at the same optical density (0.05) at the same excitation wavelength.

Transmission Electron Microscopy (TEM). The TEM images of the QDs were obtained using a JEOL JSM-890 at 200 KV to analyze their average size and size distribution. Low-coverage samples were prepared by placing a drop of a dilute hexane dispersion of QDs on a copper grid (300 mesh) coated with an amorphous carbon film.

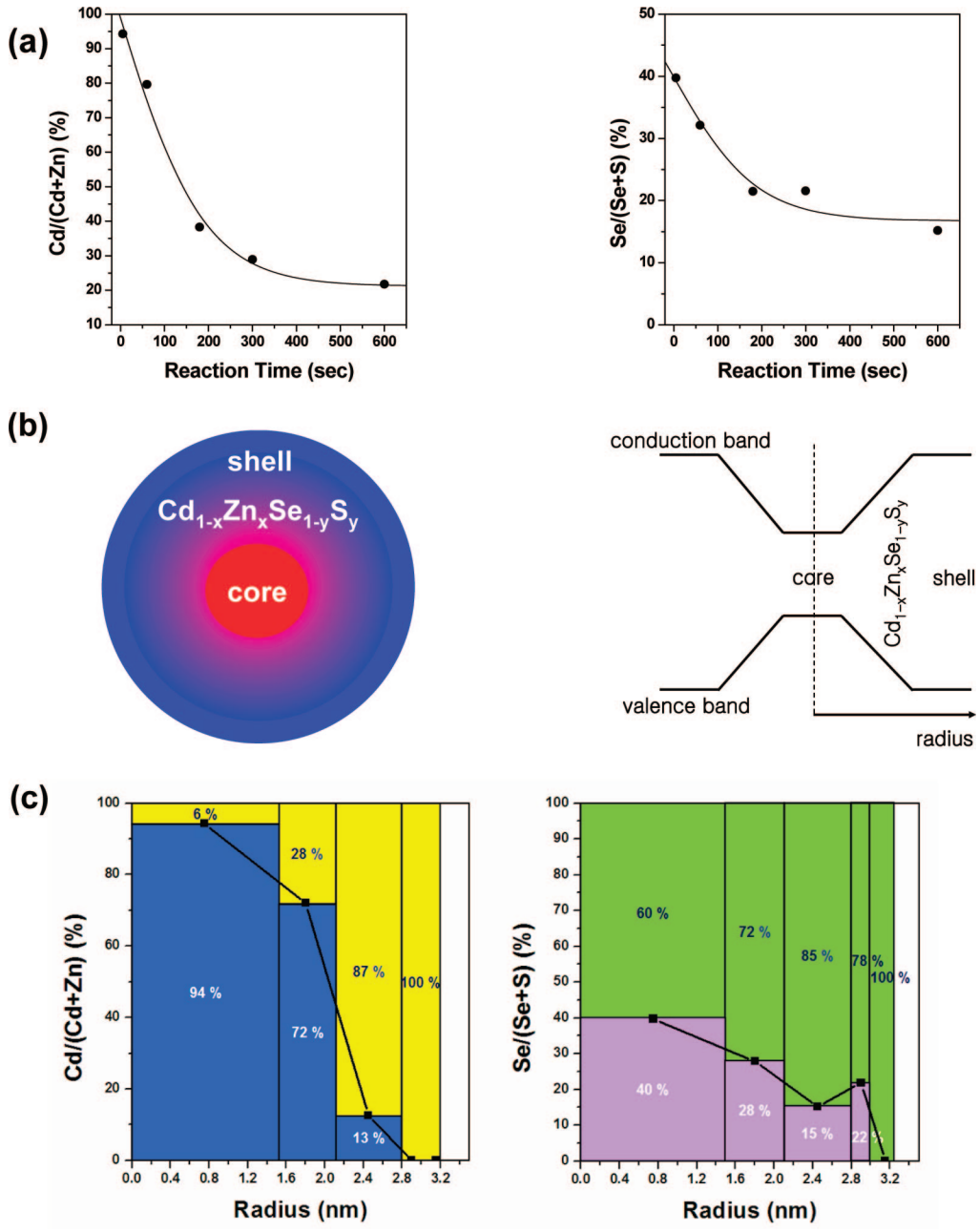

Figure 2. (a) Composition ratios of Cd-to-Zn and Se-to-S as a function of reaction time and (b) a schematic of the chemical composition (or electronic energy level) within a quantum dot. (c) Ratio of Cd or Zn to (Cd + Zn) and that of Se or S to Se/(Se + S) for each shell from the center of the quantum dot. Relative values of each component (Cd, Zn, Se, and S) in each shell are shown.

Inductively Coupled Plasma−Atomic Emission Spectroscopy (ICP-AES). An ICP-AES spectrum was measured using a Shimadzu ICPS-1000IV to analyze the elemental chemical composition of the QDs. All the samples were prepared by dissolving the QDs in 2% of HNO_3 solutions.

Powder X-ray Diffraction (XRD). X-ray powder diffraction patterns of the QDs were collected on a Brukner D5005 diffractometer using the Cu Kα radiation (1.5405 Å). Each sample was purified five times to remove excess organic coordinating compounds before XRD measurements.

Results and Discussion

Several techniques were combined to monitor the growth and to characterize the chemical composition of QDs. Figure 1 presents the TEM images of the QDs produced at various reaction times. The size of QDs increased from 3 nm (reaction time ~5 s) to 4.2 nm (1 min), 5.6 nm (3 min), 6 nm (5 min), and 6.3 nm (10 min) as the reaction proceeded. At each reaction time the QDs possessed a spherical shape with a narrow size distribution (σ < 5%) which reflected the uniform sizes of QDs.

In order to identify the chemical composition of the QDs, the ICP-AES spectra for the samples corresponding to the TEM images shown in Figure 1 were recorded. The elemental composition data as a function of reaction time (i.e., the sample prepared at each reaction time) are given in Figure 2a. At an early reaction stage (5 s), the amount of reacted Cd was 20 times higher than that of reacted Zn even

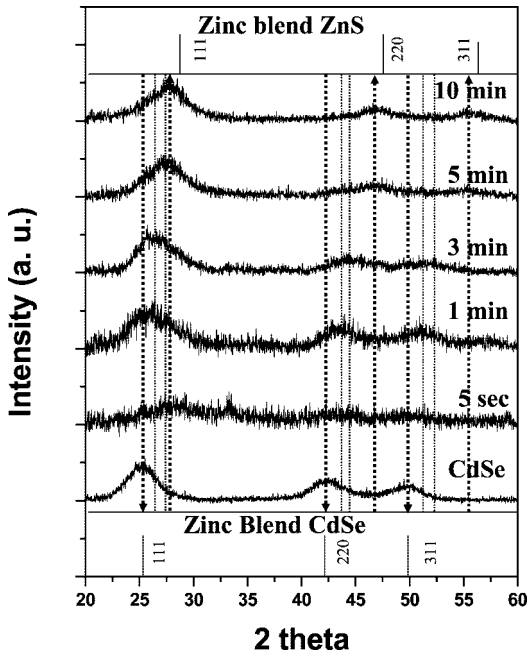

Figure 3. XRD patterns of bare CdSe and the QDs with composition gradients ($Cd_{1-x}Zn_xSe_{1-y}S_y$) obtained at 5 s, 1 min, 3 min, 5 min, and 10 min. The XRD patterns of bulk zinc-blend CdSe and ZnS are also shown at the bottom and top, respectively.

if the initial concentration of the Zn precursor was 10 times higher than that of the Cd precursor. This shows that the reactivity of the Cd precursor is much higher than that of the Zn precursor. After this 5 s period, the effect of Zn precursor on QDs increased drastically, and the amount of consumed Zn became 4 times higher than that of the Cd precursor after 10 min, at which the ratio [Cd]/([Cd] + [Zn]) started to become constant. In the case of group VI elemental chemical composition, the composition ratio of [Se] to ([Se] + [S]) at an early stage (5 s) before and after the reaction was 9% ([Se] = 0.4 mmol, [S] = 4.0 mmol) and 40%, respectively. As the reaction started, the incorporation of Se into the QDs was much faster than that of S. This indicates that the reactivity of Se is higher than that of S at the reaction temperature selected. A large amount of the Se precursor was consumed during the early stage of the reaction. As the reaction proceeded, the composition of S increased with the radius of QDs and eventually S-based layers were formed. It is clear that the core formed at the early stage of the reaction consists of Cd and Se, then Zn and S are gradually incorporated during the growth of the QDs, and finally the outer shell of the QDs are comprised of Zn and S.

The results in Figure 2a show that the composition ratio of reacted Se to S during the early stage (5 s) is lower than that of reacted Cd to Zn even though we started each reaction with the same initial concentration ratio (1:10, i.e., [Cd] = 0.4 mmol and [Zn] = 4.0 mmol, [Se] = 0.4 mmol and [S] = 4.0 mmol). We attribute this to the fact that the reactivity difference between $Cd(OA)_2$ and $Zn(OA)_2$ is higher than that between TOPSe and TOPS at the reaction temperature selected (300 °C). In Figure 2b, the drawing on the left shows the schematic for the chemical composition gradient of QDs ($Cd_{1-x}Zn_xSe_{1-y}S_y$) as a function of radius. The core is composed of Cd and Se; their amounts decrease radially outward, whereas the amounts of Zn and S increase. In Figure 2b, the drawing on the right shows the energy diagram according to the chemical composition variation. The band gap of QDs increases with the radius because of the gradual incorporation of Zn and S into the growing QDs. The QDs produced by our single-step synthesis have a core/shell structure with chemical composition (or energy) gradient. By using the data from Figures 1 and 2b, we estimated the quantitative composition profile of the QDs, which is shown in Figure 2c. Cd- and Se (and/or S)-based cores are formed first, and Zn- and S-based shells are formed successively. A Se precursor that is more reactive than the S precursor was used in the solution of 10 times lower concentration. We carried out the reaction either with 0.4 mmol of Cd and 0.4 mmol of Se or 4.4 mmol of Cd and 4.4 mmol of Se. We measured the PL of the QDs prepared by using only Cd and Se at the same reaction interval as the QDs with composition gradient. The maximum peak intensity of the PL after 200 s remains almost steady. This suggests that the Cd consumption in either 0.4 mmol of Cd and 0.4 mmol of Se or 4.4 mmol of Cd and 4.4 mmol of Se reaches a steady state after 200 s. The reactivity of Cd is so high that it reacts with Se as long as Cd and Se exist. In addition, we carried out the reaction with 0.4 mmol of Cd, 0.4 mmol of Se, 4 mmol of Zn, and 4 mmol of S. The maximum peak intensity of the PL is more blue-shifted than that of the QDs prepared using 0.4 mmol of Cd and 0.4 mmol of Se alone. This is due to the reaction of Zn and S involved in the CdSe-based core growth to some extent, which is shown in Figure 2c.

The crystallinities of the QDs were investigated using powder XRD. We synthesized bare CdSe QDs with Cd and Se precursors alone under the same conditions as we produced the QDs with composition gradients. The XRD pattern of the bare CdSe QDs is shown in Figure 3 (denoted with CdSe). The XRD patterns of the QDs with composition gradients obtained at 5 s, 1 min, 3 min, 5 min, and 10 min (denoted with 5 s, 1 min, 3 min, 5 min, and 10 min, respectively) are shown in Figure 3. The XRD patterns of bulk zinc-blend CdSe and ZnS are also shown at the bottom and top, respectively, in Figure 3. The bare CdSe QDs exhibit the zinc-blend structure. The CdSe core of the QDs with composition gradients also has the zinc-blend structure. The peaks of the QDs with composition gradients shift to higher angles as the reaction time increases, which correspond to the growth of the QDs with composition gradient ($Cd_{1-x}Zn_xSe_{1-y}S_y$). The QDs grow in all directions while maintaining the spherical shape throughout the reaction. They exhibit high PL quantum efficiency and stability, which are guaranteed by the uniform passivation over the entire surface.

Figure 4a shows the room temperature UV–vis absorption and photoluminescence (PL) spectra of the QDs obtained at various reaction times (5 s, 1 min, 3 min, 5 min, and 10 min). These are the absorption and PL spectra of the same samples shown in Figure 1. All samples have a common feature: a UV–vis absorption spectrum displays multiple excitonic peaks, and a luminescence spectrum reveals a single and narrow Gaussian-shaped PL peak with a full width at half-maximum (fwhm) narrower than 35 nm. This indicates

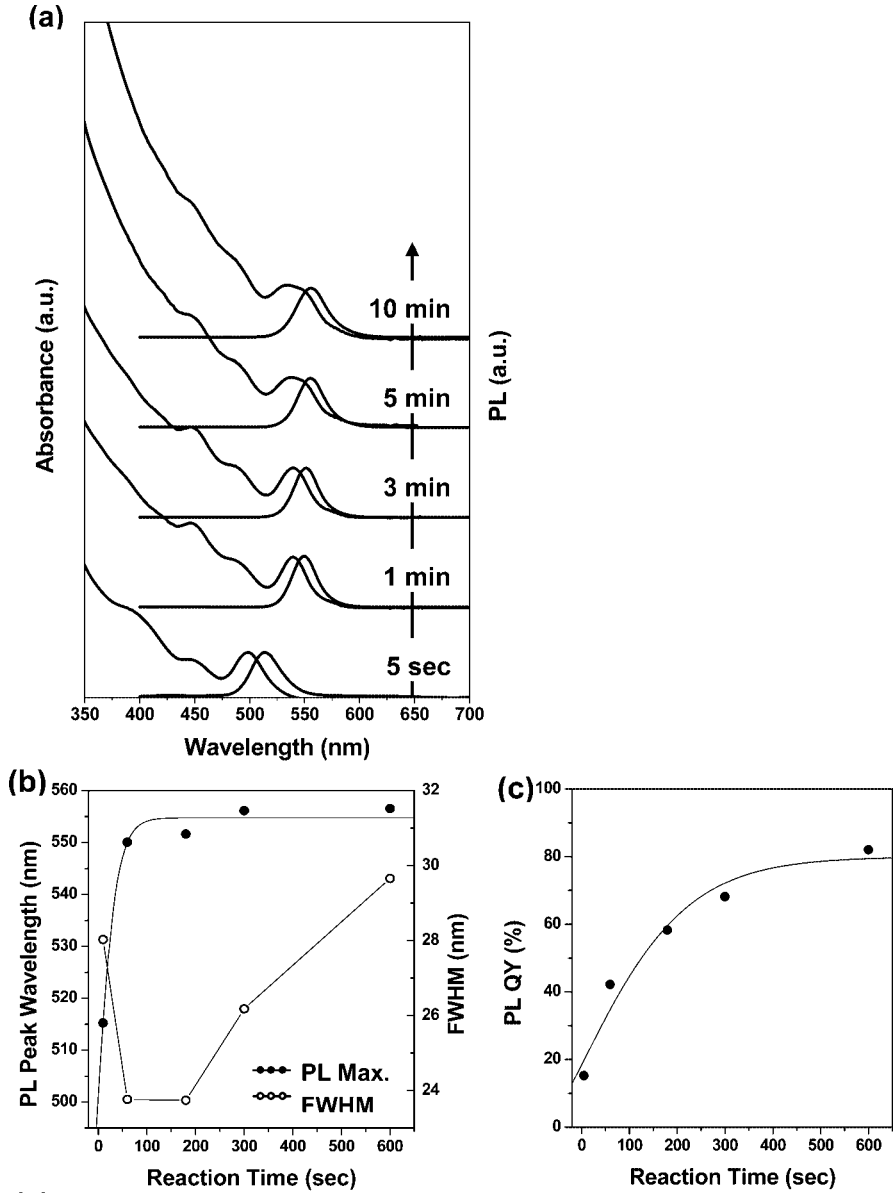

Figure 4. (a) Room temperature UV–vis absorbance and luminescence spectra for $[Cd_{1-x}Zn_xSe_{1-y}S_y]$ QDs prepared at different reaction times. (b) Peak wavelength and fwhm in PL for samples prepared at different times. (c) PL QYs of QDs prepared as a function of reaction time.

that the QDs obtained at each reaction time are uniform in size and shape and therefore uniform in the chemical composition. This result is consistent with their TEM analysis: the TEM images reveal that they are uniform in size and shape. Figure 4a shows the room temperature absorbance and luminescence spectra for a reaction time series of samples $[Cd_{1-x}Zn_xSe_{1-y}S_y]$. As shown in Figure 4a, b, the first absorption peak and the PL peak of the QDs after 1 min reaction time are red-shifted by 35 nm each relative to those of the QDs after 5 s reaction time. After 1 min of reaction time, the first absorption peak and the PL peak of the QDs after 3 min reaction time are red-shifted by 2 nm each relative to those of the QDs after 1 min reaction time, and those of the QDs after 5 min reaction time are red-shifted by 3 nm each relative to those of the QDs after 3 min reaction time. After 5 min of reaction time, there are no more red shifts in the first absorption peak and the PL peak of the QDs. These shifts reflect an increased leakage of excitons into the layers with gradual chemical composition gradient to a certain thickness. Energy gradient shells with lower band gap are initially formed and energy gradient shells with larger band gap are formed later. The initially formed energy gradient shells are responsible for the drastic red shift of PL emission. As the reaction continues further, the peak of PL emission hardly changes because the leakage of carriers to shells is suppressed by the outer shells of larger band gap, which blocks the tunneling of carriers outward. We examined the reproducibility of this method (single-step synthesis) through experiments several times and found that the changes in the PL peak position were within the less than 2 nm.

Figure 4c shows the PL quantum yield (QY) of the QDs produced at various reaction times. The room temperature PL QY increases gradually from 10% (5 s sample) to 80% (10 min sample) as the reaction proceeds. This is due to the effective passivation of the surface-state traps[15–19] of growing cores of the QDs in terms of the strain-relieved shells with chemical composition gradient. In a previous synthesis of the CdSe/ZnS core/shell structured QDs with a discrete

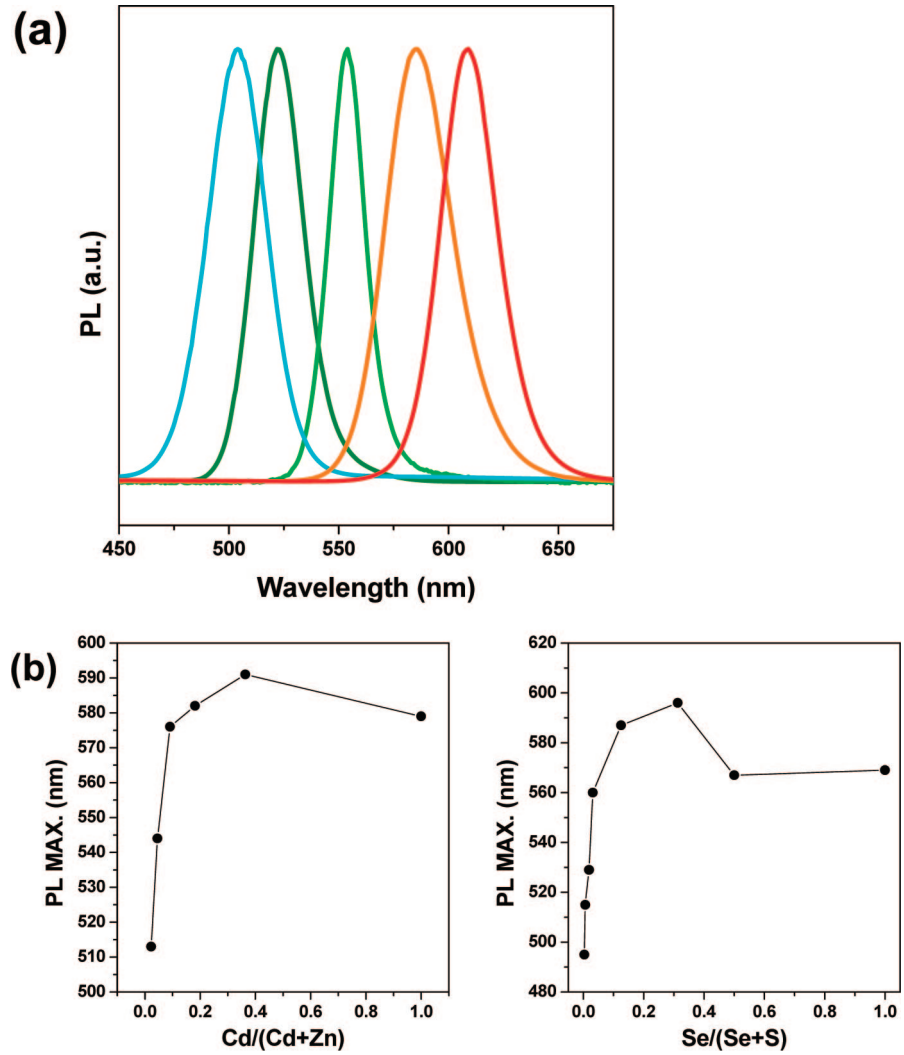

Figure 5. (a) Room temperature photoemission for different QDs prepared by the single-step synthesis method. (b) PL peak wavelengths of QDs prepared after 10 min of reaction time as a function of the initial chemical composition ratios of both Cd-to-Zn and Se-to-S.

interface, the QY increased at the first 1−2 layers of ZnS (less than 0.7 nm) and then decreased as the shell thickness increased due to the formation of defects induced by the lattice mismatch between the CdSe core and the ZnS shell.[15] However, in our approach, the QDs with chemical composition gradient exhibited a gradual increase in the QY to a thickness of about 1.5 nm. This is due to the successive relaxation of strain via chemical composition gradient. The strain may originate from the lattice mismatch between layers if the interface between the core and the shell is abrupt. Furthermore, the QDs have energy gradient in the radial direction as a consequence of the chemical composition gradient so that electrons and holes can be funneled into the core and confined to the core efficiently (carrier funneling concept).[20] As a result of the effective passivation by our approach, i.e., single-step synthesis of QDs with chemical composition (or energy) gradient, the QDs exhibited strong PL even at an elevated temperature (300 °C) during the reaction when they were illuminated using a UV lamp.

Figure 5a shows the emission wavelengths of the QDs produced by changing the relative amounts of Cd, Zn, Se, and S. The emission wavelengths range from 500 to 610 nm. The initial precursor composition corresponding to each peak from the left shown in Figure 5a is (Cd 0.4 mmol; Zn 4 mmol; Se 0.025 mmol; S 4 mmol), (Cd 0.4 mmol; Zn 4 mmol; Se 0.1 mmol; S 4 mmol), (Cd 0.4 mmol; Zn 4 mmol; Se 0.4 mmol; S 4 mmol), (Cd 0.4 mmol; Zn 4 mmol; Se 0.4 mmol; S 2.9 mmol), and (Cd 0.4 mmol; Zn 4 mmol; Se 1 mmol; S 2.3 mmol), respectively. The reactivity of Cd is the highest among Cd, Zn, Se, and S. As long as Cd exists, it will react with Se or S to form the core. With a higher concentration of Cd, the core CdSeS is larger and red-shifted. The peak shift is caused by the change in the core size of the QDs. Furthermore, in order to investigate the close correlation between the initial concentration of precursors and the PL emission wavelength of the QDs, we varied the feed ratio of group II precursors or that of group VI precursors (i.e., $0.02 < \mathrm{Cd}/(\mathrm{Cd} + \mathrm{Zn})$ or $\mathrm{Se}/(\mathrm{Se} + \mathrm{S}) < 1$) with fixed total concentration (i.e., [Cd] + [Zn] = 4.4 mmol, [Se] + [S] = 4.4 mmol). As shown Figure 5b, with the variation of the initial concentration of the Cd precursor from 0.1 to 1.6 mmol (i.e., $0.02 < \mathrm{Cd}/(\mathrm{Cd} + \mathrm{Zn}) < 0.4$), the PL peak of the QDs (acquired after 10 min of reaction in every variation) changed from 510 to 590 nm. However, a concentration of Cd from 1.6 to 4.4 mmol (i.e., $0.4 < \mathrm{Cd}/(\mathrm{Cd} + \mathrm{Zn}) < 1$) caused the PL peak to shift to shorter

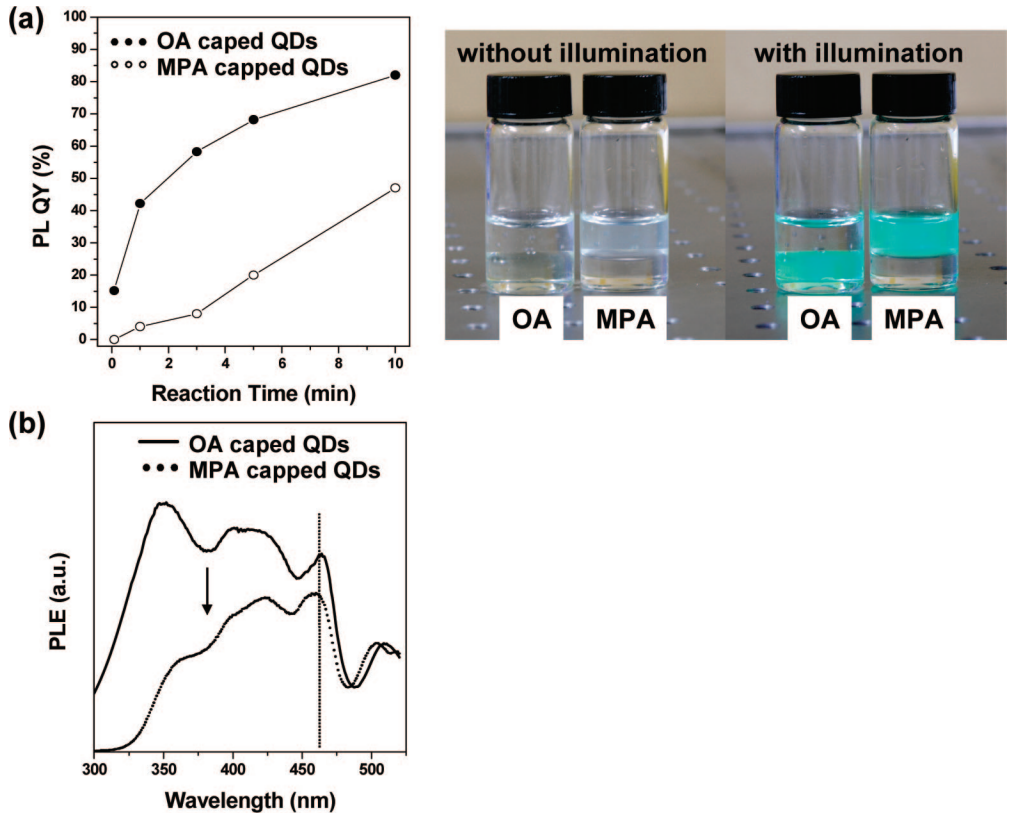

Figure 6. (a) PL QYs of oleic acid-capped (OA-capped) QDs dispersed in chloroform (denoted with solid circles, ●) and mercaptopropionic acid-capped (MPA-capped) QDs dispersed in water (denoted with empty circles, ○) prepared at different reaction times (5 s, 1 min, 3 min, 5 min, 10 min) (top left) and photographs of OA-capped QDs dispered into chloroform mixed with pure water solvent and MPA-capped QDs dispered into water of pH = 8 mixed with pure chloroform solvent. Two separate layers are formed in each case. OA-capped QDs are located in the chloroform layer (bottom half in a vial) and MPA-capped QDs in the aqueous layer (top half in a vial). (b) PLE spectra of OA-capped QDs dispersed in chloroform (solid lines) and MPA-capped QDs dispersed in water of pH 8 (dashed line).

wavelength of 570 nm even though all other reaction parameters such as the amounts of surfactants and reaction temperature remained the same. The same tendency was also observed with the variation of the amounts of Se and S. With the variation of the initial concentration of Se from 0.1 to 1 mmol (i.e., $0.02 < \mathrm{Se}/(\mathrm{Se} + \mathrm{S}) < 0.2$), the PL peak of the QDs also changed from 495 to 596 nm with the increasing incorporation of Se. However, a concentration of Se from 1 to 4.4 mmol ($0.2 < \mathrm{Se}/(\mathrm{Se} + \mathrm{S}) < 1$), with all other parameters remaining the same, caused the PL peak to shift to the shorter wavelength of 570 nm. The shift to the shorter wavelength of the PL peak may be due to the following reason. As the initial concentration of Cd and Se increases, the number of newly generated nuclei increases instead of the existing QDs growing larger; this leads to a higher concentration of QDs with the smaller cores. In order to check this, we selected the QDs with different compositions but similar emission wavelength (i.e., the QDs with $\mathrm{Se}/(\mathrm{Se} + \mathrm{S}) = 0.03$ or 1.0, as shown in Figure 5b) and compared the optical density of the QDs with $\mathrm{Se}/(\mathrm{Se} + \mathrm{S}) = 0.03$ with that of the QDs with $\mathrm{Se}/(\mathrm{Se} + \mathrm{S}) = 1.0$. The first absorption peak was used as the basis for comparison.[24] The optical density of the QDs synthesized with $\mathrm{Se}/(\mathrm{Se} + \mathrm{S}) = 1.0$ (the first exciton peak = 550 nm) was 2 times higher than that of the QDs synthesized with $\mathrm{Se}/(\mathrm{Se} + \mathrm{S}) = 0.03$ (the first exciton peak = 548 nm). This indicates that the concentration of QDs produced with $\mathrm{Se}/(\mathrm{Se} + \mathrm{S}) = 1.0$ is 2 times higher than that synthesized with $\mathrm{Se}/(\mathrm{Se} + \mathrm{S}) = 0.03$. In addition, from the TEM analysis of the QDs, we found that the QDs in all cases had similar final sizes (6.5−7 nm). The peak of PL of the QDs strongly depends on both the size and chemical composition of the core of the QDs. This finding assures that an increase in the concentration of [Cd] and [Se] only does not guarantee the QDs with larger core part (i.e., QDs with longer wavelength of PL). From these results we must take the composition ratios of Cd to Zn and Se to S into accounts to control the emission wavelength of QDs by our approach—single-step synthesis of QDs with chemical composition gradient. As we change the initial concentration ratio of Cd to Zn above 0.3 with the ratio of Se to S fixed at 0.1 (i.e., as the amount of Cd increases), the room temperature PL QY of the QDs decreases to less than 2%. This may be because the core/shell structure is not properly formed. However, the QDs produced from any combination of the concentration between Se and S with the ratio of Cd to Zn fixed at 0.1 show strong luminescence and photostability even at elevated temperature (300 °C). We attribute this to the fact that the reactivity difference between $Cd(OA)_2$ and $Zn(OA)_2$ is higher than that between TOPSe and TOPS at the reaction temperature selected, and thus the Cd-rich core with smaller band gap forms first and then the Zn-rich shell with larger band gap forms later. This results in the

(24) Yu, W. W.; Qu, L.; Guo, W.; Peng, X. *Chem. Mater.* **2003**, *15*, 2854–2860.

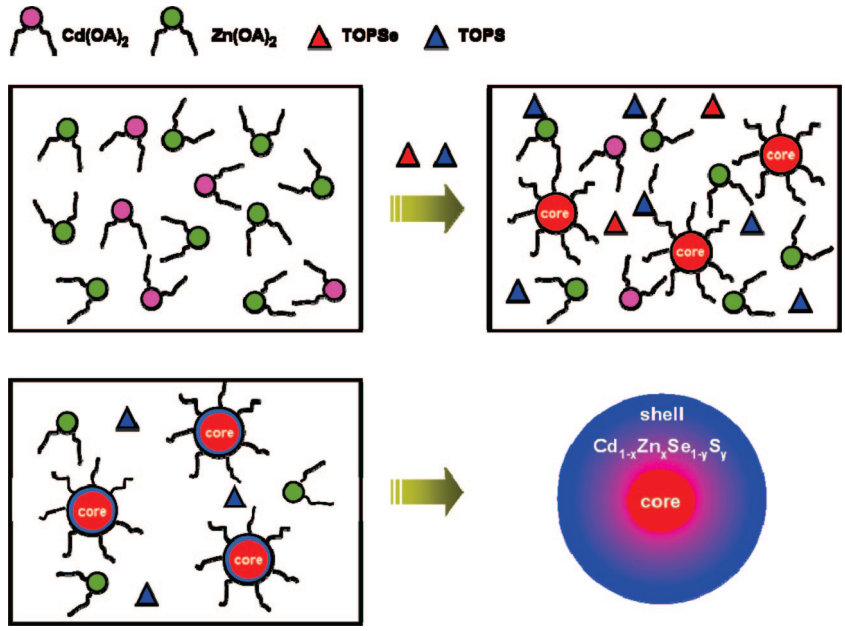

Figure 7. Schematic of the possible reaction mechanism for the single-step synthesis of QDs with chemical composition gradients.

energy gradient in the radial direction in the QDs. This energy gradient helps the electrons and holes to be confined and funnel into the core of the QDs. This is why the QDs with the energy gradient structure have a high PL QY. In our composition gradient QDs, the low quantum efficiency of QDs is related to surface passivation rather than the CdSe core formation. This is because the quantum efficiency of the QDs obtained at an early stage (less than 1 min) shows almost same quantum efficiency regardless of any initial Cd to Zn ratios, but that of the QDs obtained after certain reaction time shows different quantum efficiency depending on the initial Cd to Zn ratios. Small amounts of Zn (i.e., Cd to Zn ratio of 0.1) are not sufficient for the effective surface passiviation of the QD, and this leads to low quantum efficiency.

Biological applications require water-soluble quantum dots. The optoelectronic applications require the surface passivation of QDs as well. We surface-passivate the QDs with mercaptopropionic acid (MPA) in order to make them water-soluble. We measured the QYs of the QDs of 5 s reaction time(i.e., QDs produced after the reaction time of 5 s), 1 min reaction time, 3 min reaction time, 5 min reaction time, and 10 min reaction time as they were produced or later surface-passivated with MPA, respectively. Theses QY data are shown in Figure 6a. The QDs as produced by single-step synthesis with chemical gradient were originally surface-passivated with oleic acid that functioned as a solvent and coordinating ligand. After surface modification with MPA, the QYs of all the QDs of 5 s reaction time to 10 min reaction time decreased compared with those of the as-produced QDs (i.e., originally surface-passivated with OA). The room temperature PL QY of the surface-passivated QDs of 10 min reaction time with MPA was 50%. QDs of longer reaction time have a thicker gradient shell that prevents electrons and holes from leaking to surface trap sites, which may be formed during the surface-passivation process. Figure 6b shows the photoluminescence excitation (PLE) spectra of QDs before and after surface modification with MPA. After surface modification with MPA, the intensity of the PLE spectrum in the wavelengths shorter than 460 nm decreased significantly (indicated with an arrow), whereas that of the PLE spectrum in the wavelengths longer than 460 nm decreased slightly. This can be explained as follows: the electrons and holes excited by low-energy photons are confined to the core of the QDs and are more probable to form luminescing excitons, whereas the electrons and holes excited by high-energy photons are created in the outer part of the QDs with energy gradient and can easily leak out to the surface; thus, they have higher chances of tunneling out to the surface trap sites, producing lower PL. It is well-known that surface states are formed during the surface modification of QDs with MPA, and they lead to the nonradiative decays of excitons. The excitons generated by excitation with wavelength above 460 nm are created in the cores of smaller energy gap and are confined in the cores energetically lower than composition (energy) gradient shells which effectively protect them from nonradiative decays. Therefore, the PLE spectra in the longer wavelength region above 460 nm do not show difference between OA-capped and MPA-capped QDs. On the other hand, the excitons generated by excitation with shorter wavelength below 460 nm are created in the shells as well as in the cores; thus, they have more chances of leaking out to the surface states of the QDs for the MPA-capped QDs. Therefore, the PLE intensity of MPA-capped QDs decreases drastically in the shorter wavelength region below 460 nm.

On the basis of the results mentioned above, we can produce QDs with chemical (or energy) gradient by single-step synthesis using the different reactivity of precursors at the reaction temperature selected. The single-step synthesis of QDs with chemical composition gradient was possible due to the proper choice of reaction temperature and surfactants (OA for group II elements and TOP for group VI elements) and different chemical reactivity of the precur-

sors. The mechanism for the formation of QDs with chemical composition gradient is traced as follows: nucleation is mainly driven by Cd and Se, and the spontaneous growth of a shell with chemical composition gradient is driven by Zn and S. This is shown in Figure 7. This is because the precursors with larger ionicity bind strongly with surfactants and thus have low reactivity. Zn-OA and S-TOP have higher binding energy and thus lower reactivity compared with Cd-OA and Se-TOP, respectively. The layers with composition gradient relieve the strain caused by the lattice mismatch between the CdSe core and the ZnS shell; consequently, the gradual change in composition ensures high luminescence even if the thickness of the outer part of the QDs is more than two atomic layers. Furthermore, the outer shell consists of ZnS of a larger band gap;[25] therefore, it effectively confines excitons to the core. This structure will enhance PL. As a result of the sequential reactions of precursors in single-step synthesis of QDs with chemical composition gradient, the QDs have chemical composition (or energy) gradient, a smaller band gap in the core and a larger band gap in the shell, which provides confinement and funneling of holes and electrons to the core, reduction of defects due to lattice mismatch, photostability, and high PL. Our approach—single-step synthesis of QDs with chemical composition gradient—will be a new method to produce highly luminescent and photostable semiconductor QDs in an efficient manner.

(25) Phillips, J. C.; Van Vechten, J. A. *Phys. Rev. Lett.* **1969**, *22*, 705–708.

Summary

QDs with various emission wavelengths (500−610 nm) were synthesized by a low-cost and simple method using the difference in the reactivity of precursors at the reaction temperature selected. We named this method as single-step synthesis of QDs with chemical composition (or energy) gradient. The QDs produced using this method have chemical composition (or energy) gradient which relieves the strain caused by the lattice mismatch between the CdSe core and the ZnS shell; therefore, a gradual change in composition ensures high luminescence of the QDs. The chemical composition (or energy) gradient in the QDs helps the confinement of carriers (electron or hole) to the core and the funneling of carriers into the core; thus, it enhances the PL QY and the photostability of the QDs. Highly luminescent QDs can be produced on a large scale using the single-step synthesis with chemical composition gradients. We also produced water-soluble QDs by surface passivating them with MPA. Further, we demonstrated that these QDs could also be applied for optoelectronic materials or devices by suitably surface passivating them.

Acknowledgment. This research was supported in part by MOE through BK21 program and Seoul R&BD program. We thank KOSEF and the Center for Nanotubes & Nanostructured Composites for supporting this research. We also acknowledge the financial support from KOSEF through Nano Systems Institute, National Core Research Center.

CM070754D